

Controlled Nanoporous Structures of a Marine Diatom

Kazuo Umemura^{1,*}, Xing Liao², Shigeki Mayama³, and Mohammed Gad⁴

¹Tokyo Tech-Tsinghua University Joint Graduate Program, Tokyo Institute of Technology,
Tsinghua University, Beijing 100084, China

²Tsinghua University, Beijing 100084, China

³Tokyo Gakugei University, Koganei, Tokyo 184-8511, Japan

⁴Microbiology Department, Faculty of Science, Ain-Shams University, Abbaseya 11566, Cairo, Egypt

We demonstrated chemical etching of a marine diatom shell with 1 N NaOH for controlling the pore size of nanoporous structures of the shell under various conditions. Scanning electron microscopy (SEM) images clearly revealed that the pore size of the diatom shells was regulated in the case of etching at 25 °C. In contrast, fluctuations in the etched structures was relatively high even during short periods degradation at 40, 60, and 90 °C; therefore, controlled nanoporous structures could not be fabricated. This is the first example of artificial modification of natural diatom shells at the nanoscale although diatom shells have been widely used in industry. In addition, a backbone-like structure was observed during the etching process. The structure was similar to the intermediate structure observed during the primitive stage of the diatom cell growth. Probably, this information is valuable for studying the mechanism of nanoporous structures of diatoms.

Keywords: Diatom Shell, Nanoporous, Silica, Etching, Bioceramics.

1. INTRODUCTION

Diatoms are one of the most common photosynthetic microalgae in nature.¹⁻⁴ They exist wherever light and water are available. They have a unique box-shaped cell wall or frustules, which is made of hydrated silica.¹⁻³ The cell wall of diatoms is one of the most typical bioceramic materials. The wall is decorated with ornamentations of various shapes that range from rib-like structures to well-organized nanoporous holes. For this reason, fossil diatoms have been widely used as filters, plasters, and so on.

Although there are many artificial nanoporous materials, nanoporous structures of diatoms are quite unique. According to the growth of diatom cells in low-energy environments involving limited sunlight (e.g., seas, rivers, or lakes), the structures can be spontaneously fabricated.⁴⁻⁷ Such a fabrication mechanism of nanostructures can be very rarely found in artificial nanomaterials such as carbon nanotubes. Furthermore, because diatom shells are bioceramics made of silica and organic molecules such as polyamine, they can be naturally recycled.⁵⁻⁷ The application of the biological system of formation of nanoporous structures to nonbiological nanomaterials fabrication can lead to substantial advances in nanotechnology. For these reasons, many researchers have been interested in the nanostructures of diatoms and their formation processes.

For example, atomic force microscopy (AFM) and scanning electron microscopy (SEM) of diatoms have been reported in order to characterise diatoms at the nanoscale.⁸⁻¹² However, no example exists of artificial control of nanoporous diatom structures. In nanoscopic studies and industrial applications, natural diatom shells were employed without modification.

We consider that if the nanoporous structures of a diatom shell can be artificially controlled, the range of industrial applications of diatom shells can be considerably increased. For example, the functioning of water filters can be controlled by controlling the pore size of diatom shells. Here, we demonstrated the controlling of the pore size of a diatom shell. A diatom shell was chemically etched under various conditions in order to control the shell structures. The etched structures were examined by optical microscopy and SEM.

2. MATERIALS AND METHODS

2.1. Preparation of Diatom Shells

A marine diatom, *Navicula sp.*, was cultured using a Daigo IMK culture medium (Nihon Pharmaceutical Co., Ltd., Osaka, Japan) in old sea water. One mM Na₂SiO₃ (Wako, Japan) was added to the culture medium as the Si source. After culturing for more than two weeks, the culture medium was replaced with pure water by centrifugation

*Author to whom correspondence should be addressed.

(4000 rpm \times 10 min, five times). Diatom shells were then extracted from the living diatoms by a previously described procedure.^{13,14} Finally, the solvent was replaced with pure water by centrifugation (4000 rpm \times 10 min, eight times).

2.2. Etching of Diatom Shells

A diatom suspension was well stirred and then 400 μ l of the suspension was rapidly introduced into sample tubes. Then, 100 μ l of 5 N NaOH was added to each sample tube (final concentration of 1 N) and stirred well. In the case of the control sample, 100 μ l of pure water was added to a diatom suspension. The mixture was incubated at 25, 40, 60, or 90 $^{\circ}$ C for 5, 15, 30, or 60 min. After the incubation, 100 μ l of 5 N HCl was added in order to stop degradation; the solvent was then rapidly replaced with water by centrifugation (10000 rpm \times 5 min, eight times) in order to remove chemicals.

2.3. Electron Microscopy

Ten μ l of diatom suspension was dropped on a glass or mica surface and then dried in air. Prior to dropping the diatom suspension, the mica surface was modified with 3-aminopropyltriethoxysilane (APS) in order to obtain a hydrophobic surface.¹⁵ The samples were coated with platinum using an ion sputter (JFC-1100, JEOL, Tokyo, Japan) at 5 mA for 5 min. The thickness of the platinum coating was 10–20 nm. A commercially available scanning electron microscope (JSM-6301F, JEOL, Tokyo, Japan) was employed for structural characterization. The cell length and pore size were directly measured from the obtained SEM images.

3. RESULTS AND DISCUSSION

Figure 1 shows the diatom shells before and after etching observed by SEM with a low magnification (\times 400). Macroscopically, it is clear that most of the diatom shells did not collapse after etching. The length of the diatom shells measured from the SEM images was 17.1 ± 2.4 , 17.2 ± 1.4 , and 16.7 ± 1.4 μ m for etching durations of 0, 5, and 15 min at 25 $^{\circ}$ C, respectively (Fig. 2). The length marginally decreased after 15 min; however, no drastic change was observed before and after etching. Although whole body of a diatom shell not only nanopores must be dissolved by NaOH, the shape of the shell was successfully kept at these conditions.

Figure 3 shows the highly magnified SEM images of similar samples. The nanopores of diatom shells are clearly observed. The SEM images reveal that the pore sizes increase with the etching period. A magnified image of the etched sample shows that each pore has a clear edge without any jagged unevenness (Fig. 3(D)). The regions with no pores in Figures 3(A–C) are the centres of the

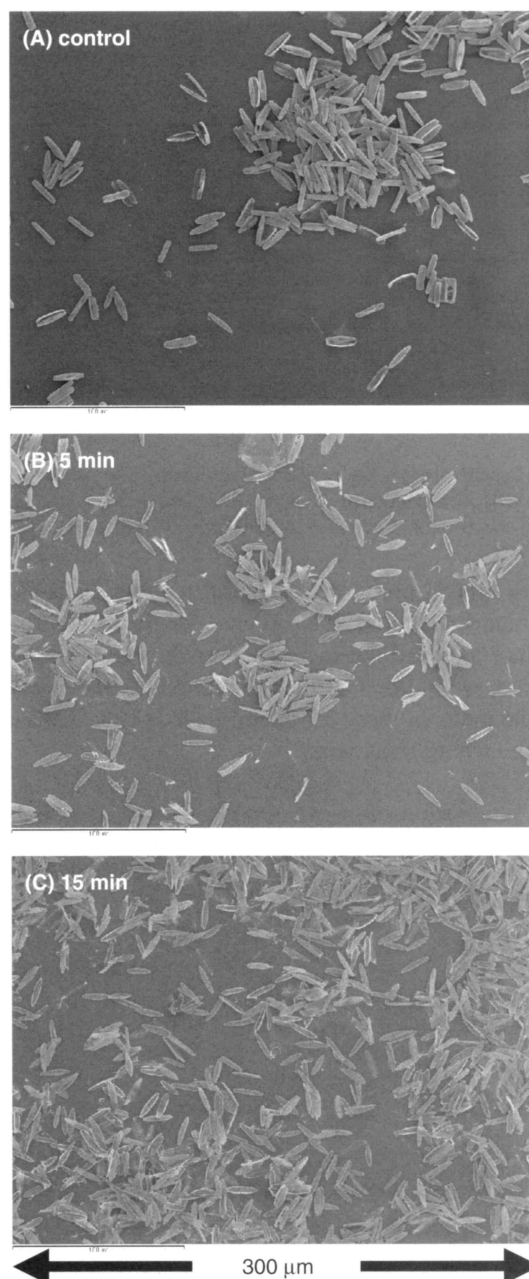


Fig. 1. SEM images of diatom shells decomposed at 25 $^{\circ}$ C. (A) Control (not decomposed). (B) and (C) 5 min and 15 min at 25 $^{\circ}$ C, respectively. The lateral lengths of the images are 300 μ m.

diatom shell. Except these regions, nanopores are seen on the entire surface of the diatom shells.

The size of the nanopores was measured from the SEM images of several diatom shells as the length of the major and minor axes of each pore (Fig. 4). The pores that were located from the second line to the fourth line were measured in order to compare various samples in the same area. Because diatoms are living beings, the original pore sizes fluctuate marginally. For using diatoms in filters or other devices, the device properties are probably decided by the most typical pore shape. Therefore, we compared

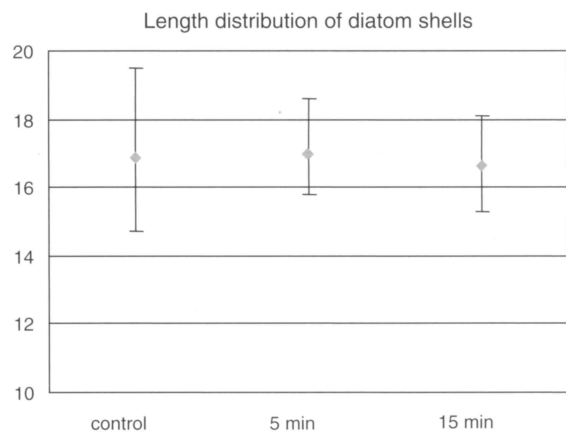


Fig. 2. Length distribution of the diatom shells. The length of the diatom shells were measured from the SEM images. The degradation condition was control, 5 min and 15 min at 25 °C from left to right.

the most typical pores at the central regions. In our data, the standard deviation value of the lengths of the major and minor axes did not increase after the etching process. Therefore, we notice that the fluctuations in the pore size are in the range of those for the original diatom shells even after the etching treatment.

The length of the major axis was 215, 237, and 273 nm for etching durations of 0, 5, and 15 min, respectively. The length increased to 22 and 37 nm for the first 5 min and the next 10 min, respectively. The length of the minor axis was 81, 98, and 121 nm for etching durations of 0, 5, and 15 min, respectively. The length increased to 17 and 24 nm for the first 5 min and the next 10 min, respectively. The data suggested that the nanoporous structures of diatom shells were successfully regulated by this method as well as non-biological ceramic materials. Mechanism of non-biological silica has been reported previously.^{16, 17} In alkaline condition, solid SiO_2 is easily dissolved as H_4SiO_4 .¹⁶ SiOSiOH on an amorphous silica surface is separated to SiOH and $\text{Si(ONa)}_2(\text{OH})_2$ after reacting with 2NaOH .¹⁷ After all, Si atoms are gradually peeled from the surface. We think that etching mechanism of a diatom frustule can be explained with the same way.

However, the etching manner of a diatom shell is not completely same as that of non-organic uniform silica. The data suggests that the etching speed was slightly greater at the beginning of the etching process in both major and minor axes. We consider two possibilities. (1) The pore edges might be thinner than the other areas and (2) The composition of the pore edges was different from

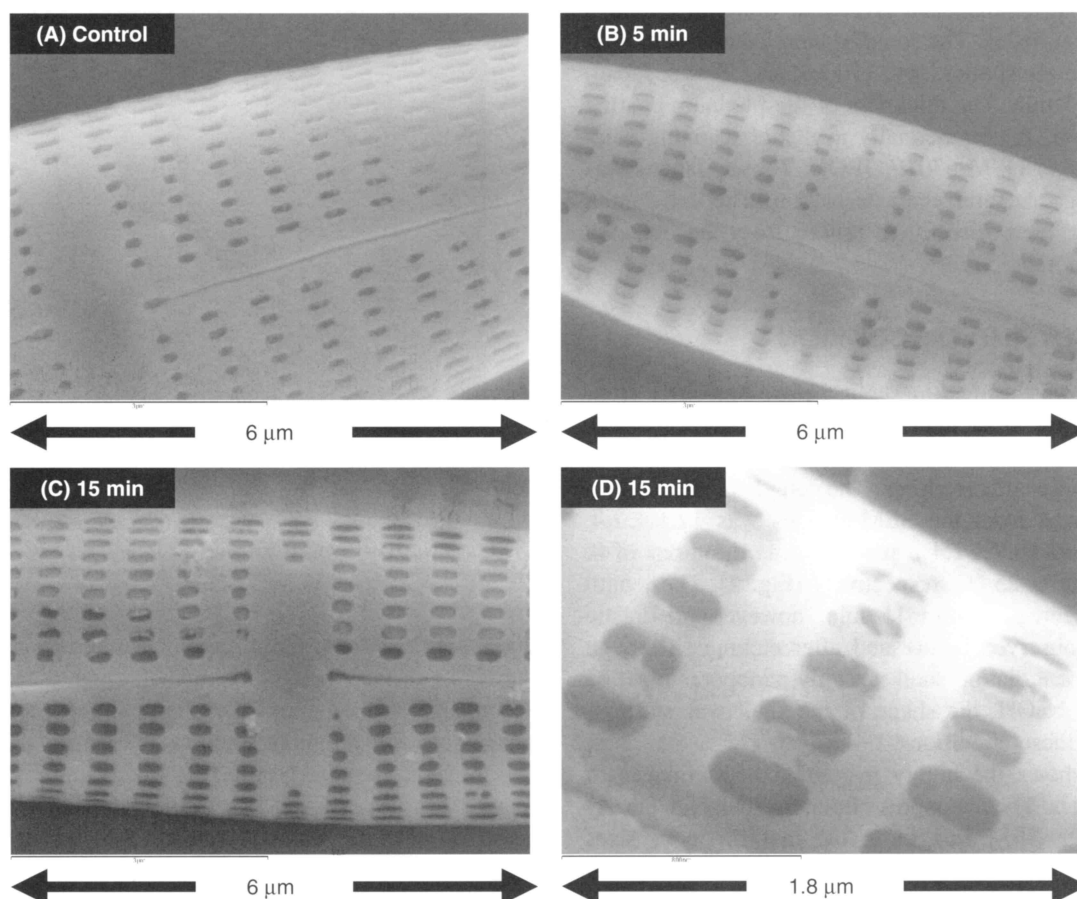


Fig. 3. SEM images of diatom shells etched at 25 °C. (A) Control (not etched). (B) 5 min. (C and D) 15 min. Lateral length of each image. (A), (B), and (C): 6 μm . (D): 1.8 μm .

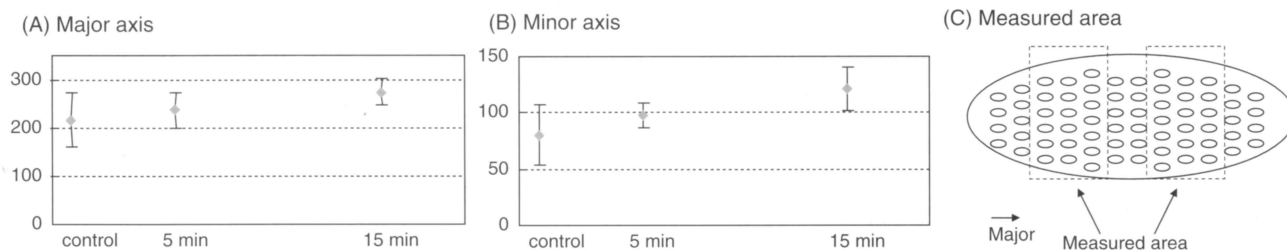


Fig. 4. Size distribution of nanopores on diatom shells. (A) Length of major axis. (B) Length of minor axis. Degradation condition was control, 5 min and 15 min at 25 °C from left to right. (C) Schematic view of pore size measurement. Pores between six lines in the square boxes were measured and plotted.

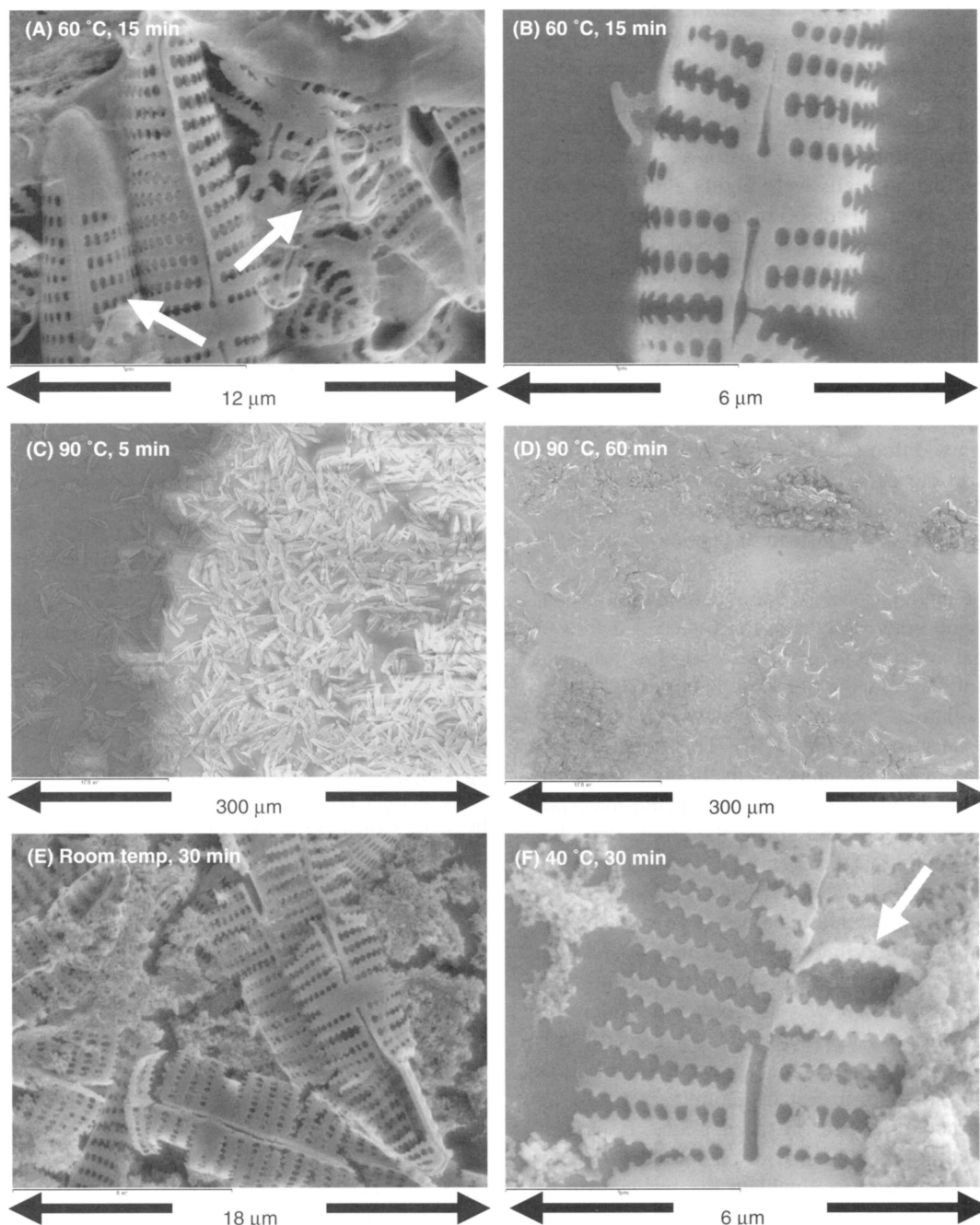


Fig. 5. SEM images of diatom shells decomposed under various conditions. (A) and (B) 15 min at 60 °C. (C) 5 min at 90 °C. (D) 60 min at 90 °C. (E) 30 min at 25 °C. (F) 30 min at 40 °C. Lateral length of the images is 12, 6, 300, 300, 18, and 6 mm from (A)–(F), respectively.

that of the other areas. It is difficult to consider that NaOH was lost within 5 min because diatom shells can be completely degraded in 1 N NaOH in the following experiments (see Fig. 5(D)).

We examined the etching of diatom shells under different conditions. When the diatom shells were etched at 60 °C, considerable fluctuations were observed in the structures of the diatom shells. Some of the shells exhibited oriented nanopores, whereas others exhibited collapsed structures (indicated by arrows in Fig. 5(A)). Figure 5(B) shows a diatom shell in the intermediate stage of structural collapse. It suggests that fluctuations in the diatom shell structures are relatively high. It can be concluded that low temperatures are suitable for controlling the etching process of diatom shells.

In the case of etching at 90 °C, regulation of the diatom shell structures was impossible. Even for a 5 min incubation period, the diatom shells were highly aggregated. No clear object was observed for 60-min degradation period, although obscure materials were observed (Fig. 5(D)). Even though a similar sample was observed by an optical microscope, it was impossible to find any diatom shells. It was known that pure silica can be extracted when diatom shells are incubated in 10% NaOH at 90 °C for 60 min.¹⁸ Although whether the diatom shells were completely decomposed or not was not mentioned, it was suggested that the condition is sufficient to extract silica from diatom shells. In our experiments, when the diatom shells were etched for a 30-min incubation period, a backbone-like structure was observed instead of pores even at 25 °C (Fig. 5(E)).

Although the main purpose of our experiments was controlling the nanoporous structures, the obtained data provided additional information; one interesting fact was with regard to the softness of a diatom shell. In our experiments, some of the collapsed diatom shells showed a bent style (indicated by the arrow in Fig. 5(F)). This suggests that silica in the diatom shell exhibits relatively high viscoelasticity. The diatom shell is composed of organic materials such as polyamine along with silica; therefore, it probably has a relatively higher viscoelasticity when compared with that of normal glass. The mechanical properties of a diatom shell at the nanoscale have not been studied thus far. Our results suggested that a nanomechanical study on diatom shells is probably an interesting research subject.

A backbone-like structure was also observed under several different conditions (Figs. 5(A), (B), (E), and (F)). It is known that backbone like structures appear at the primitive stage of diatom shell formation in nature.^{19,20} If similar intermediate structures appear in the degradation process in a reverse order, it probably provides helpful information for fundamental research to elucidate the mechanism of nanoporous structures of diatom shells. Further, analysis

of detailed structures of the etched frustules such as thickness of the shell is the next important research target although SEM pictures did not give us quantitative information about it.

4. CONCLUSION

Diatom nanoporous structures were successfully controlled by an etching process. The data suggests that slow degradation at 25 °C provides the best results. The obtained data also included helpful information for fundamental research of diatom shell formation. We hope that our results will be useful in increasing the range of industrial applications of diatom shells.

Acknowledgments: We thank Mr. Yasufumi Nakashima (Tokyo Institute of Technology), Prof. Xin-Hui Xing (Tsinghua University) and Prof. Xiaozhong Zhang (Tsinghua University) for providing instruments and supporting the experiments. We also thank Dr. Hiroshi Sekiguchi (Tokyo Institute of Technology) for his helpful advice. One of the authors wishes to thank the Musashi Institute of Technology for providing an opportunity to stay at Tsinghua University.

References and Notes

1. F. Round, R. Crawford, and D. Mann, *The Diatoms*, Cambridge University Press, Cambridge, UK (1990).
2. M. Sumper and E. Brunner, *Adv. Funct. Mater.* 16, 17 (2006).
3. P. J. Lopez, J. Desclés, A. E. Allen, and C. Bowler, *Curr. Opin. Biotechnol.* 16, 180 (2005).
4. R. C. Dugdale and F. P. Wikerson, *Nature* 391, 270 (1998).
5. N. Kröger, R. Deutzmann, C. Bergsdorf, and M. Sumper, *Proc. Nat. Aca. Sci. USA* 97, 133 (2000).
6. N. Kröger, S. Lorenz, E. Brunner, and M. Sumper, *Science* 298, 584 (2002).
7. N. Poulsen, M. Sumper, and N. Kröger, *Proc. Nat. Aca. Sci. USA* 100, 12079 (2003).
8. F. Noll, M. Sumper, and N. Hampp, *Nano. Lett.* 2, 91 (2002).
9. S. Komura, *Diatom* 12, 7 (1996).
10. I. C. Gebeshuber, J. H. Kindt, J. B. Thompson, Y. Delamo, H. Stachelberger, M. A. Brzezinski, G. D. Stucky, D. E. Morse, and P. K. Hansma, *J. Microscopy* 212, Pt 3, 292 (2003).
11. J. C. Weaver, L. I. Pietrasanta, N. Hedin, B. F. Chmelka, P. K. Hansma, and D. E. Morse, *J. Struct. Biol.* 144, 271 (2003).
12. M. J. Higgins, J. E. Sader, P. Mulvaney, and R. Wetherbee, *J. Phycol.* 39, 722 (2003).
13. T. Nagumo and H. Kobayashi, *Diatom* 5, 45 (1990).
14. T. Nagumo, *Diatom* 10, 88 (1995).
15. K. Umemura, M. Ishikawa, and R. Kuroda, *Anal. Biochem.* 290, 232 (2001).
16. W. Stumm, *Chemistry of the Solid-Water Interface*, A Wiley-Interscience Publication, New York, USA (1992).
17. T. Ichikawa and H. Koizumi, *J. Nucl. Sci. Technol.* 39, 880 (2002).
18. T. Nishiyama, JPN Patent Application No. 2001-97711 (2001).
19. S. Mayama and H. Kobayashi, *Diatom Res.* 4, 111 (1989).
20. S. Mayama and A. Kuriyama, *J. Plant Res.* 115, 289 (2002).

Received: 19 October 2006. Revised/Accepted: 22 December 2006.